이학석사학위논문

Explosive percolation transitions in growing networks

성장하는 네트워크에서의 폭발적 여과 상전이

2016년 2월

서울대학교 대학원
물리·천문학부
오수민

Abstract

Explosive percolation transitions in growing networks

SooMin Oh
Department of Physics and Astronomy
The Graduate School
Seoul National University

Recent extensive studies of the explosive percolation (EP) model revealed that the EP transition is of second order with extremely small value of the order parameter exponent β. This result was obtained from static random networks, in which the number of nodes in the system remains constant during the evolution of the network. However, on-line social networks, where the giant component among the members grows quickly, can be growing networks, in which the number of nodes in the system is increased with time steps. Thus, one needs to study EP transitions occurring in growing networks. Here we study a general case in which the number of node candidates that are selected at each time step is given as m. When $m = 2$, this model reduces to an existing model that is the ordinary percolation model in growing networks, which undergoes an infinite-order transition. When $m \geq 3$, however, we find that the transition becomes second order due to the suppression effect against the growth of large clusters. Using the rate equation approach and Monte Carlo simulations, we show that the exponent β decreases algebraically with increasing m, whereas it decreases exponentially for static networks.

Keywords : Percolation transition, Spanning cluster, Explosive percolation transition, Discontinuous percolation transition, Achlioptas process, Finite size scaling theory

Student Number : 2012-20372

Contents

List of figures

List of tables

Chapter 1

Introduction

1.1 Percolation

In statistical physics, percolation theory helps to understand the emergence of a giant component as links are occupied with a certain probability between each pair of nodes in a system [1, 2] and phase transitions in non-equilibrium systems. This simple model has been applied to a variety of real-world phenomena such as the sol-gel transition [3–6], spreading of epidemic diseases [7–10], and the metal-insulator transition [11]. Conventionally, a percolation transition is second-order [1, 2]; however, interest in other types of percolation transitions such as first-order [12], infinite-order [13, 14] or mixed-order [15] phase transitions has increased recently. This trend has been triggered by the explosive percolation (EP) model [16] under the Achlioptas process in static networks. These Achlioptas processes, choosing a pair which minimizes the size of the resulting cluster among m candidate nodes, suppresses the formation of large clusters. It delays the phase transition point and then the explosive phase transition arises. Many physicists looked for the possibility that there are discontinuous phase transition models like k-core percolation models [15, 17–19] and invented study the explosive percolation models. For example, there are cascading failure model in interdependent networks [20, 21], the spanning clusteravoiding(SCA) model [22], synchronization transition model [23], jamming transition model [24] and so on.

Now, we recall a percolation model in growing networks, which exhibits an infinite-order phase transition [14]. In this model, at each time step, a node is added to the system, and then two distinct nodes are chosen randomly and connected unless they are not connected yet. The model we consider here is a generalization of the existing model [14] by applying the Achlioptas process to it. Instead of choosing two nodes, we choose m distinct nodes and identify the sizes of the components to which each selected node belongs. The two nodes that belong to the smallest two components among those m components are connected. When the two nodes belong to the same component, they are connected but the size of that component does not increase.

We investigate critical behaviors as a function of m, and show that the cluster size distribution changes drastically when the Achlioptas process is applied. When $m = 2$, the cluster size distribution follows power law not only at the transition point $p = p_c$ but also below p_c; however, when $m \geq 3$, it exhibits critical behavior only at p_c and sub-critical behavior for $p < p_c$. The EP dynamic rule leads to the suppression effect against the growth of large clusters, which results that the cluster size distribution in a large-cluster region decays exponentially. Thus, the transition is second-order. We also show that the critical exponent β associated with the order parameter decreases with m algebraically in growing networks; however, it does exponentially in static networks [25, 26]. This fact reflects that the suppression effect is weaker in growing networks than that in static networks. Moreover, we obtain the critical exponents and their tendency in both growing and static models for a general value of m. In fact, the explosive percolations in static networks were well studied in ref. [26, 27] but we rechecked this in our static network models. we expect that our studies help the development of researches in complex networks.

1.2 Percolation in Erdős-Rényi network

1.2.1 Phase transition to percolation

There are many percolation models in lattice, networks, etcetera but in this paper we focused on the percolation in networks. Networks consists of lines(edges) and nodes(vertices). In this section we introduce Erdős-Rényi (ER) networks model which is classical percolation model in network. ER networks model introduced in 1959 [29] is one of the percolation models which undergoes continuous phase transition. This ER model is the growth network model with randomly selecting two nodes to be linked at each time t and the total number of nodes N is fixed. And there is no giant cluster if the average degree $\langle k \rangle$ is less than 1 in the limit $N \to \infty$ [28]. However, the giant cluster emerges at $\langle k \rangle = 1$ and its size monotonically increases as $\langle k \rangle$ increases with the order parameter(the relative size of the giant cluster) critical exponent $\beta = 1$.

1.2.2 Finite size scaling ansatz and data collapse : order parameter

Now, we introduce the finite scaling methods using scaling ansatz and data collapse. For continuous phase transitions, every physical variable X near the threshold t_c is scale-free due to the infinite correlation length of the system at t_c [31, 32], so it has a power-law form $X \sim |t - t_c|^a$, where a is a critical exponent and t is time which is equivalent to link density. On a finite system of size N, any physical variable X has the following scaling ansatz form $X = N^{-a/\bar{\nu}} f[(t-t_c)N^{1/\bar{\nu}}]$ near the threshold [32, 33], where the scaling function $f(z)$ is analytic at all finite z and $\bar{\nu}$ is equal to the dimension d times the correlation exponent ν. Now, the order parameter

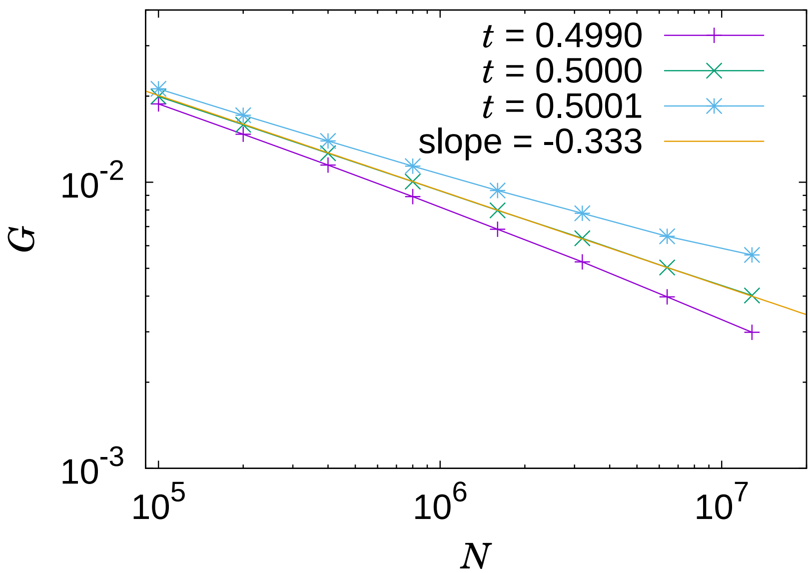

Fig. 1.1: (Color online) Log-log plot of G versus N at different t. It is well described by power law at $t_c = 0.5000(1)$, $\beta/\bar{\nu} = 0.333(1)$.

$G_N(t)$ is the relative size of the largest cluster in a system with N fixed nodes at time t. The critical exponent of the $G_N(t)$ is β and the scaling ansatz is $G_N(t) = N^{-\beta/\bar{\nu}} g[(t-t_c)N^{1/\bar{\nu}}]$, where the scaling function $g(z)$ is analytic at all finite z.

And we numerically observed the order parameter $G_N(t)$ are made when $N/10^4 = 2^6, 2^7, 2^8, 2^9$, and 2^{10}. Measures are averaged over more than 10^5 ensembles. If we use the correct t_c, $G_N(t)$ must show the power-law behavior $N^{-\beta/\bar{\nu}}$. We investigate it and find that $t_c = 0.5000(1)$ and $\beta/\bar{\nu} = 0.333(1)$ [see fig. 1.1]. And using $t_c = 0.5000(1)$ and $\beta/\bar{\nu} = 0.333(1)$, we try to make the curves for various system size collapse to finite size scaling form of $G_N(t)$ as shown fig. 1.2. From this analysis, we found $1/\bar{\nu} = 0.333(1)$ and it gives us the order parameter exponent $\beta = 1.00(3)$.

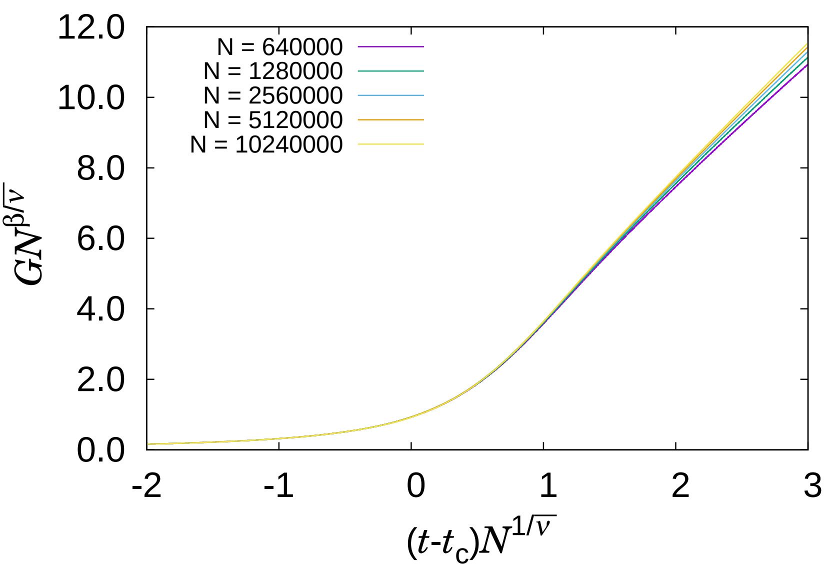

Fig. 1.2: (Color online) Finite-size scaling collapse using $G_N(t) = N^{-\beta/\bar{\nu}} f((t-t_c)N^{1/\bar{\nu}})$ It shows best fit with $1/\bar{\nu} = 0.333(1)$ when $\beta/\bar{\nu} = 0.333(1)$.

1.2.3 Finite size scaling ansatz and data collapse : average cluster size

The average cluster size $\langle s \rangle$ is obtained from the cluster size distribution as $\langle s \rangle = \sum_{s=1}^{s*} s^2 n_s(t)$, where $n_s(t)$ is the relative number of cluster of size s and $s*$ is limited to finite clusters. This value behaves like the susceptibility. The critical exponent of the $\langle s \rangle$ is γ and the scaling ansatz is $\langle s \rangle = N^{\gamma/\bar{\nu}} h[(t - t_c)N^{1/\bar{\nu}}]$, where the scaling function $h(z)$ is analytic at all finite z. And we numerically observed the order parameter $G_N(t)$ are made when $N/10^4 = 2^7, 2^8, 2^9$, and 2^{10}. Measures are averaged over more than 10^5 ensembles. And using $t_c = 0.5000(1)$ and $1/\bar{\nu} = 0.333(1)$, we try to make the curves for various system size collapse to finite size scaling form of $\langle s \rangle$ as shown

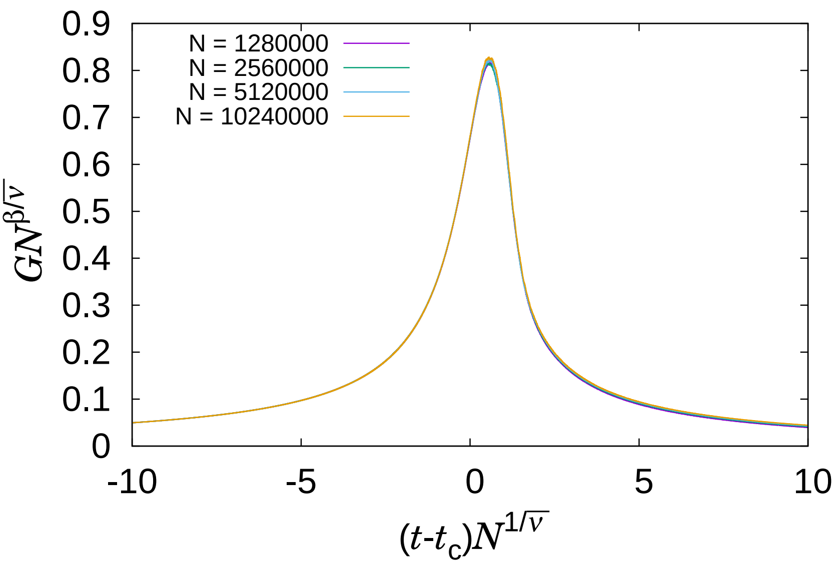

Fig. 1.3: (Color online) Finite-size scaling collapse using $\langle s \rangle = N^{\gamma/\bar{\nu}} h[(t - t_c)N^{1/\bar{\nu}}]$ It shows best fit with $1/\bar{\nu} = 0.333(1)$ when $\gamma = 1.00(5)$.

fig. 1.3. From this analysis, we found the average cluster size exponent $\gamma = 1.00(5)$.

1.2.4 Finite size scaling ansatz and data collapse : cluster size density

For all cluster sizes $s \ll s_\xi$, the cluster size distribution $n_s(t)$ decay as a power law in s, that is $n_s(t) \sim s^{-\tau}$, while decaying faster than a power law for $s \gg s_\xi$. Now when $t \to t_c$ and $s \gg s_\xi$, we propose the following scaling ansatz $n_s(t) \sim s^{-\tau}\exp(-s/s_\xi)$ for $n_s(t)$, where the characteristic cluster size s_ξ diverges as a power law with critical exponent $-1/\sigma$ in term of the distance of t from t_c, that is, $s_\xi \sim |t-t_c|^{-1/\sigma}$ [31]. Then we can know that $n_s(t)$ follow scaling function ansatz $n_s(t) \sim s^{-\tau}\exp(-s|t-t_c|^{1/\sigma})$.

And we numerically observed the order parameter $n_s(t)$ are made when $N = 10^7$ and measures are averaged over more than 10^5 ensembles. If we

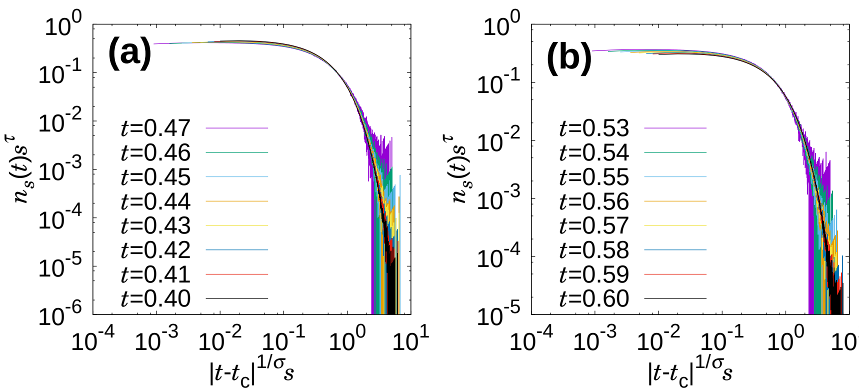

Fig. 1.4: (Color online) Data collapse plots of the rescaled cluster size distribution $n_s(t)s^\tau$ versus $s|t-t_c|^{1/\sigma}$ for different time steps when (a) $t < t_c$ and (b) $t > t_c$, where $\tau = 2.50(1)$ and $\sigma = 0.50(1)$.

use the correct t_c, $n_s(t)$ must show the power-law behavior $s^{-\tau}$. Using $t_c = 0.5000(1)$, we found that $\tau = 2.50(1)$ and we try to make the curves for various t collapse to finite size scaling form of $n_s(t)$ as shown fig. 1.4. From this analysis, we found $\sigma = 0.50(1)$.

Chapter 2

Two models: the growing and the static network models

In this paper, we consider two types of network models, growing and static. In a growing network, the number of nodes increases one by one at each time step, whereas in a static model, the number of nodes remains fixed from the beginning. Links are added one by one at each time step in both models according the following rules:

(i) A growing networks begins with isolated nodes in a system. At each time step, a node is added in the system and then m candidate nodes are selected randomly. At time t, when the number of nodes $N(t) = 1 + t$ is less than m, all of the nodes are selected as candidates. Next m clusters are identified for each selected node. Some of clusters may be identical when they contain more than one selected nodes. The two smallest clusters are selected among the m clusters, and the corresponding nodes are identified and connected with probability p if they are not already connected. When $m = 2$, this growing network model reduces to the exponentially growing network model, which was proposed by Callaway et al. [14].

(ii) For the static network model, N nodes are present from the beginning and remain fixed. At each time step, m candidate nodes are selected uniformly at random, and the sizes of the respective clusters where they belong are identified. The two nodes corresponding to the two smallest clusters are connected with probability one. When $m = 2$, this static network model reduces to the Erdős-Rényi (ER) random network model [29].

Chapter 3

Rate equation approach for the cluster size distribution

3.1 Growing network model with $m = 3$

Let $n_s(p,t)$ be the cluster number density of size s at time t, where p denotes the probability that a links is connected between two selected nodes. The rate equation of $n_s(p,t)$ is given by

$$\begin{aligned}\frac{d(N(t)n_s)}{dt} = p\Bigg[& \sum_{i+j=s;i<j} 3in_i\left(jn_j\right)^2 \\ & + \sum_{i+j=s;i<j} 6in_i jn_j c_{j+1} \\ & + \left(\frac{s}{2}n_{\frac{s}{2}}\right)^3 + 3\left(\frac{s}{2}n_{\frac{s}{2}}\right)^2\left(c_{\frac{s}{2}+1}\right) \\ & - 2\left(sn_s\right)^3 - 6\left(sn_s\right)^2 c_{s+1} - 3\left(sn_s\right)^2\left(1-c_s\right) \\ & - 3sn_s\left(c_{s+1}\right)^2 - 6sn_s\left(1-c_s\right)c_{s+1}\Bigg] + \delta_{1s},\end{aligned} \tag{3.1}$$

where n_i denotes $n_i(p,t)$ and $c_s(p,t) = 1 - \sum_{i<s} in_i(p,t)$ to simplify the notation. The first term of the right hand side of Eq. (3.1) comes from merging two clusters of size i and j with $i < j$, which produces a cluster of size $s = i + j$. One node is selected from a cluster of size i and the other two nodes are selected from either one cluster of size j or two distinct clusters of the same size j. For simplicity, this process is denoted by $(i, j > i, j > i)_{i+j=s}$. Similarly, each term is obtained from the merging process as follows: for the second term, $(i, j > i, k > j)_{i+j=s}$, the third, $(\frac{s}{2}, \frac{s}{2}, \frac{s}{2})$, the fourth, $(\frac{s}{2}, \frac{s}{2}, i > \frac{s}{2})$. The third and fourth terms appear only when s is even. Furthermore, for the fifth term, (s, s, s), the sixth term, $(s, s, i > s)$, the seventh term, $(s, s, i < s)$, the eighth term, $(s, i > s, j > s)$, and the ninth term, $(s, i < s, j > s)$ referring to Ref. [30]. The last term δ_{1s} arises when a node is added every time step, and the factor p comes from the probability that a link is added, which causes the merging process.

Based on this rate equation, we calculate $n_s(p)$ in the steady state up to a certain size s^*, for instance, $s^* = 10^6$. Note that $n_s(p)$ decays in a power-law way as $n_s(p_c) \sim s^{-\tau}$ at a transition point p_c, and exhibits crossover behavior $n_s(p) \sim s^{-\tau} \exp(-s/s_c)$ for $p \neq p_c$ with $s_c \sim |p - p_c|^{-1/\sigma}$ [1, 2]. When $p > p_c$, an infinite cluster exists separately from the finite clusters. The percolation threshold is calculated as $p_c = 0.413842(1)$ using the criterion that $n_s(p_c)$ follows power law at p_c as shown in Fig. 3.5. Moreover, the exponent τ is determined to be $\tau \approx 2.5$. We also check the crossover behaviors for $p < p_c$ and $p > p_c$ in Fig. 3.5. The exponent σ is obtained by scaling the plots of $n_s(p)s^{\tau}$ versus $s|p - p_c|^{1/\sigma}$ for different p values. It can be shown that the data are well collapsed on a single curve when $\sigma \approx 0.72$.

Next, the order parameter is obtained using the relation, $G(p) \approx 1 - \sum_{s=1}^{s^*} s n_s(p)$ [1, 2], where s^* takes on several values to observe the effect of the artificially established cutoff values. The order parameter follows the power-law form, $G(p) \sim (p - p_c)^{\beta}$, where $\beta = 0.694(2)$. The inset of Fig. 3.7 is a double logarithmic plot of the order parameter as a function

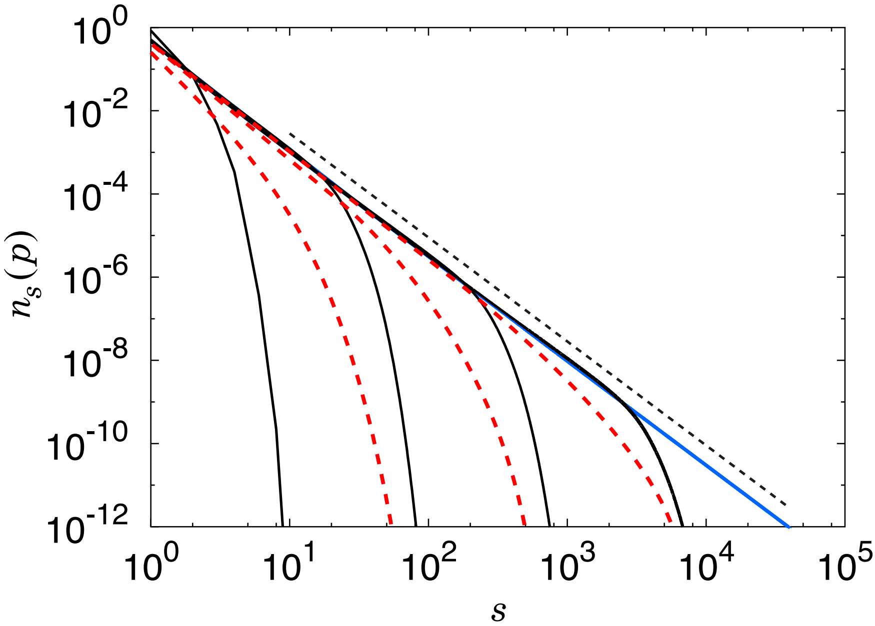

Fig. 3.5: (Color online) For growing networks with $m = 3$, plot of $n_s(p)$ vs s at $p = p_c$ (blue solid line), $p > p_c$(red dashed curves) and $p < p_c$(black solid curves) based on numerical values obtained from the rate equation. The transition point p_c is $p_c = 0.413842(1)$, and the exponent τ is approximately 2.5. The black dashed line is a guide line with slope -2.5.

of $(p - p_c)$, which exhibits power-law behavior as expected. The obtained value of β satisfies the hyperscaling relation $\beta = (\tau - 2)/\sigma$ [1, 2, 31].

The mean cluster size $\langle s \rangle$ is obtained from the cluster size distribution as $\langle s \rangle = \sum_{s=1}^{s*} s^2 n_s(p)$, which behaves like the susceptibility, $\langle s \rangle \sim (p - p_c)^{-\gamma}$ for $p > p_c$ and $(p_c - p)^{-\gamma'}$ for $p < p_c$. We also determine that $\gamma = \gamma' \approx 0.696$. The numerical values obtained from the rate equation are shown in Fig. 3.8. In the insets, $\langle s \rangle$ is plotted in double logarithmic axes as a function of $p - p_c$ for $p > p_c$, and $p_c - p$ for $p < p_c$. The exponent γ satisfies the well-known scaling relation $\gamma = (3 - \tau)/\sigma$ [1, 2].

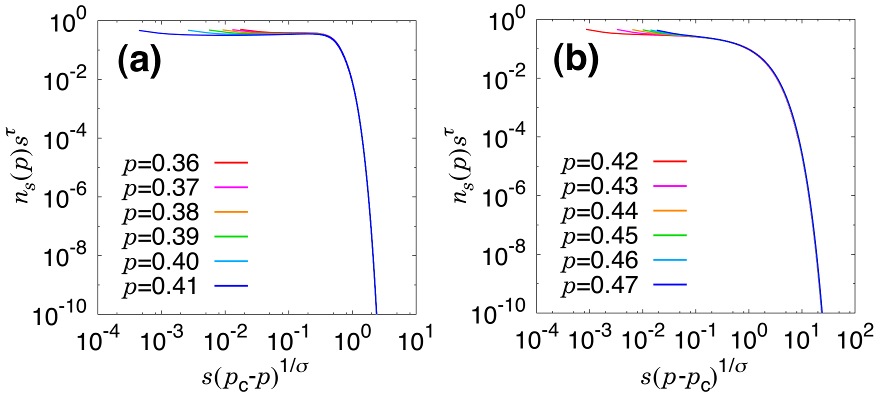

Fig. 3.6: (Color online) For growing networks with $m=3$, plot of $n_s(p)s^\tau$ versus $s|p-p_c|^{1/\sigma}$ for different values of p when (a) $p<p_c$ and (b) $p>p_c$. Data for different p values are well collapsed onto a single curve by choosing $\sigma=0.720(2)$ and $\tau=2.500(1)$.

3.2 Growing model with general m

We extend the rate equation in Eq. (3.1) for $m=3$ to arbitrary m as follows:

$$\begin{aligned}
&\frac{d(N(t)n_s)}{dt} \\
&= p\Bigg[\sum_{r=1}^{m-1} m\binom{m-1}{r-1}\sum_{i+j=s;i<j} in_i\left(jn_j\right)^{m-r}\left(c_{j+1}\right)^{r-1} \\
&+\sum_{r=1}^{m-1}\binom{m}{r-1}\left(\frac{s}{2}n_{\frac{s}{2}}\right)^{m-(r-1)}\left(c_{\frac{s}{2}+1}\right)^{r-1} \\
&-2\sum_{r=2}^{m}\binom{m}{r}\left(sn_s\right)^r\left(c_{s+1}\right)^{m-r}-m\left(sn_s\right)\left(c_{s+1}\right)^{m-1} \\
&-\sum_{r=1}^{m-1} m\binom{m-1}{r}\left(1-c_s\right)\left(sn_s\right)^r\left(c_{s+1}\right)^{m-1-r}\Bigg]+\delta_{1s}.
\end{aligned} \tag{3.2}$$

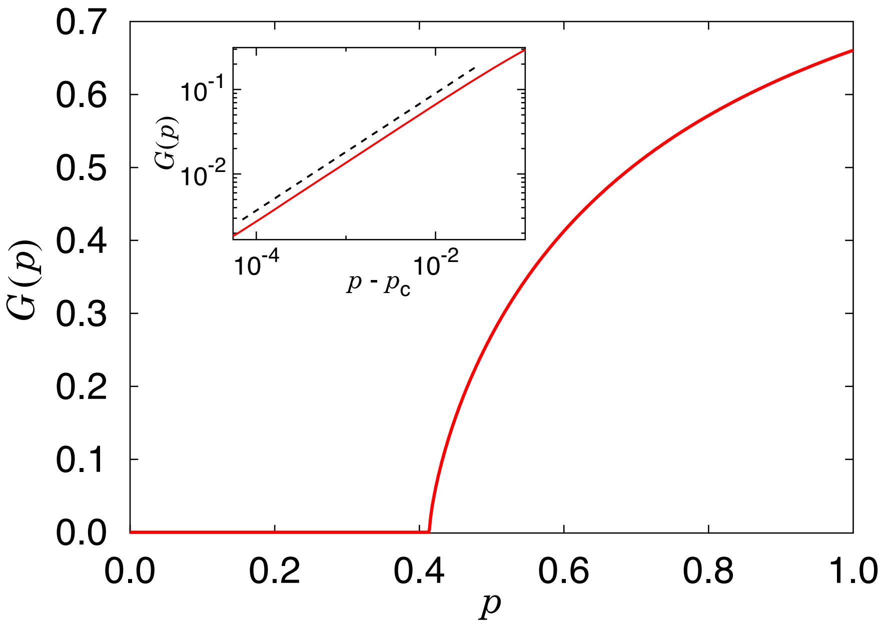

Fig. 3.7: (Color online) For growing networks with $m = 3$, plot of $G(p)$ vs p. The data points are obtained from the rate equation. Inset: The dashed line is a guide line with slope 0.694(2).

Again, the second term on the right hand side is valid only when s is even. Repeating the steps taken in the case $m = 3$, we obtain the critical exponents τ, σ, β, γ, and the percolation threshold p_c up to $m = 10$, which are listed in Table 3.1.

Following the conventional formalism for the second-oder percolation transition, we examine the scaling relation between the critical exponents and their tendencies for m candidates. Note that the critical point p_c and critical exponent β behave like $1 - p_c \approx 1.81/m$ and $\beta \approx 1/(m - 1.56)$ as shown in Fig. 3.9. However, a rigorous derivation of these formulas is still necessary. Next, we determine the exponents τ and σ for $m = 4 \cdots, 10$ by following similar steps used for $m = 3$. We find that the values are approx-

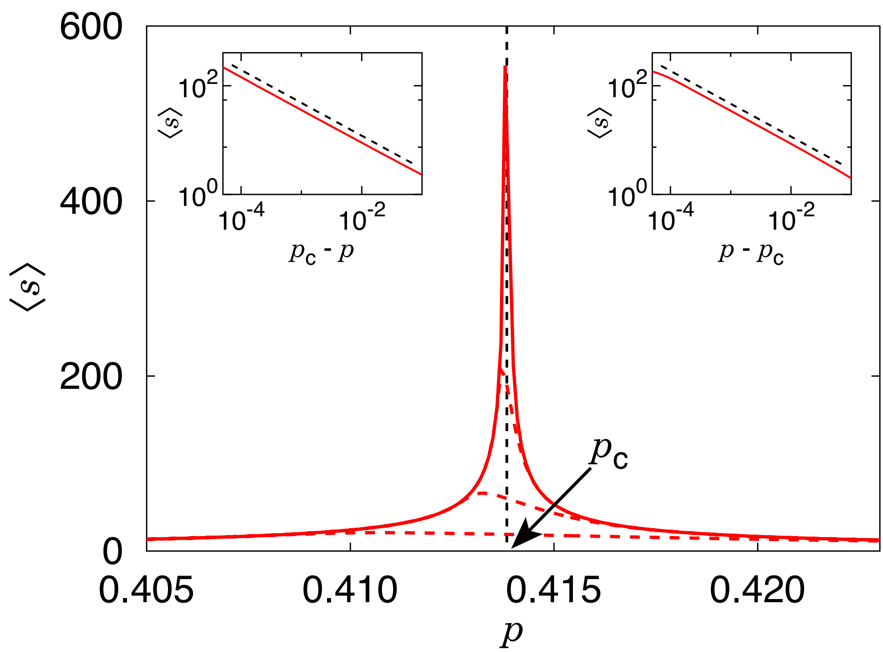

Fig. 3.8: (Color online) For growing model with $m = 3$, plot of the susceptibility, that is mean cluster size, as a function of p. The data points are obtained from the rate equation. Insets : Double logarithmic plots of $\langle s \rangle$ versus $|p - p_c|$ for $p < p_c$ (left) and $p > p_c$ (right). The dashed lines are guide lines with slope $-0.696(3)$.

imately by the formulae $\tau = 2 + 1/(m-1)$ and $1/\sigma = (m-1)\beta$ as shown in Fig. 3.10. Furthermore, we determine that $\gamma = (m-2)\beta$.

3.3 Static model with $m = 3$

We consider the evolution of static networks under the rule described in Chap. 2. In this case, the number of nodes is fixed all the way as N. The rate

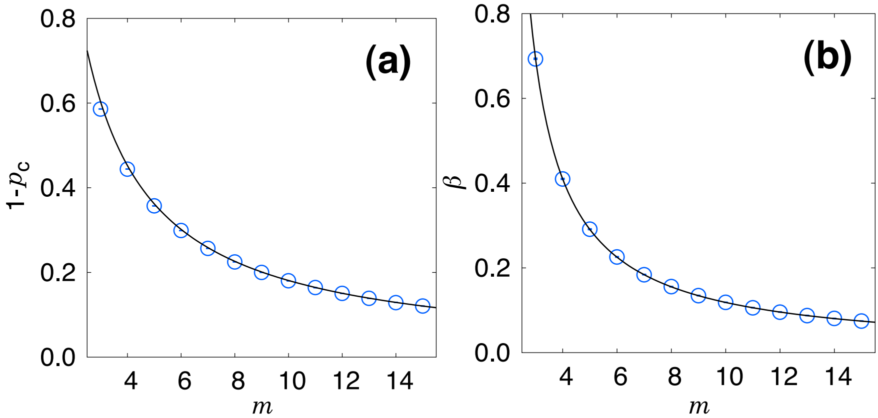

Fig. 3.9: (Color online) For growing model with general m, (a) empirical plot of $1-p_c$ versus m. Data points of $1-p_c$ for different values of m behave like the formula $1.81/m$. (b) Empirical plot of β vs m. Data points of β for different values of m behave like the formula $\beta = 1/(m-1.56)$. Note that the error bars are smaller than the symbol sizes.

equation is written as

$$\begin{aligned} N\frac{dn_s}{dt} &= \sum_{i+j=s;i<j} 3in_i\left(jn_j\right)^2 + \sum_{i+j=s;i<j} 6in_i jn_j c_{j+1} \\ &+ \left(\frac{s}{2}n_{\frac{s}{2}}\right)^3 + 3\left(\frac{s}{2}n_{\frac{s}{2}}\right)^2\left(s_{\frac{s}{2}+1}\right) \\ &- 2\left(sn_s\right)^3 - 6\left(sn_s\right)^2 c_{s+1} - 3\left(sn_s\right)^2\left(1-c_s\right) \\ &- 3sn_s\left(c_{s+1}\right)^2 - 6sn_s\left(1-c_s\right)c_{s+1}, \end{aligned} \tag{3.3}$$

where n_i denotes $n_i(t)$ and $c_s(t) = 1 - \sum_{i<s} in_i(t)$. The terms on the second line of Eq. (3.3) related with $\frac{s}{2}$ are valid only when s is even. In contrast to the growing network, there is no steady state in the size distribution, and n_s depends on t. Accordingly it takes longer time to evaluate $n_s(t)$ explicitly compared with that of the growing network model. We obtain $n_s(t)$ up to a

Table. 3.1: Numerical estimates of the percolation threshold p_c, exponent of the cluster size distribution τ, exponent of the characteristic cluster size σ, exponent of the order parameter β, and exponent of the susceptibility γ of the growing network model for $m = 3, \cdots, 10$. τ^* and β^* were obained from $\tau^* = 2 + 1/(m-1)$ and $\beta^* \approx 1/(m-1.56)$, respectively.

m	p_c	τ^*	τ	σ	β^*	β	γ
3	0.413842(1)	$\frac{5}{2}$	2.500(1)	0.720(2)	0.694	0.694(2)	0.696(3)
4	0.555873(1)	$\frac{7}{3}$	2.333(1)	0.812(2)	0.410	0.410(2)	0.813(3)
5	0.642748(1)	$\frac{9}{4}$	2.250(1)	0.858(2)	0.291	0.291(1)	0.874(6)
6	0.701282(1)	$\frac{11}{5}$	2.200(1)	0.885(2)	0.225	0.226(1)	0.904(2)
7	0.743370(1)	$\frac{13}{6}$	2.167(1)	0.905(2)	0.184	0.184(1)	0.922(2)
8	0.775078(1)	$\frac{15}{7}$	2.143(1)	0.918(2)	0.155	0.156(1)	0.934(2)
9	0.799820(1)	$\frac{17}{8}$	2.125(1)	0.928(2)	0.134	0.135(1)	0.944(3)
10	0.819663(1)	$\frac{19}{9}$	2.111(1)	0.936(2)	0.119	0.119(1)	0.950(3)

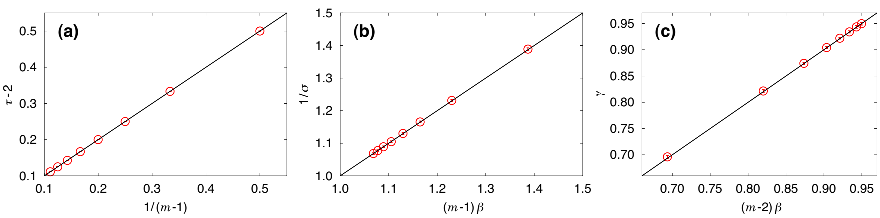

Fig. 3.10: (Color online) For growing networks with general m, formula testing for the exponents of (a) the cluster size distribution τ, (b) the characteristic cluster size σ, and (c) the mean cluster size γ, where the numerical data are obtained from the rate equation. Data are fit reasonably to the straight line predicted by the formula, and the error bars are smaller than the symbol sizes.

certain cluster size $s^* = 5 \times 10^5$.

We determine the percolation threshold t_c as shown in Fig. 3.11 by the criterion that the cluster size distribution follows power law at t_c. It is obtained that $t_c = 0.849130(1)$ and $n_s(t_c) \sim s^{-\tau}$ with $\tau \approx 2.105$. For $t < t_c$ and $t > t_c$, the cluster size distribution exhibits a crossover behavior as $n_s(t) \sim s^{-\tau} \exp(-s|t-t_c|^{1/\sigma})$. Using the data-collapse method, we obtain $\sigma \approx 0.79$ as shown in Fig. 3.12.

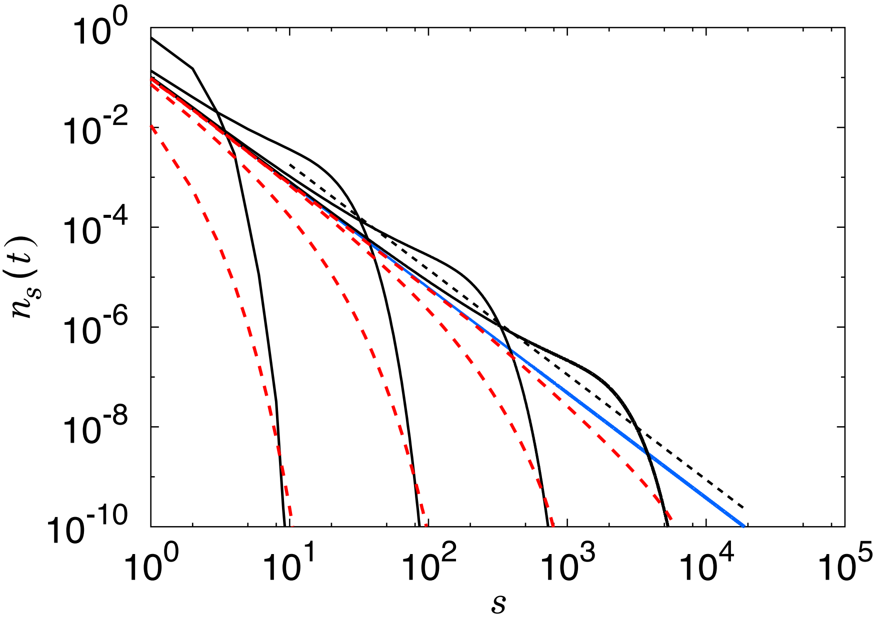

Fig. 3.11: (Color online) For static networks with $m=3$, plot of $n_s(t)$ vs s at $t=t_c$(blue solid line), $t>t_c$(red dashed curves) and $t<t_c$(black solid curves) based on the numerical values obtained from the rate equation. The transition point t_c is determined as $t_c=0.849130(1)$ and the exponent τ is determined as $\tau=2.105(5)$. Black dashed line is a guideline with slope -2.105.

Next, we consider the behavior of the order parameter $G(t)$ at time step t. The order parameter is calculated using the relation $G(t)=1-\sum_{s=1}^{s^*} sn_s(t)$. We expect that $G(t)\sim(t-t_c)^{\beta}$, and obtain $\beta=0.133(1)$ in Fig. 3.13. We also obtain the mean cluster size or the susceptibility defined as $\langle s\rangle=\sum_{s=1}^{s^*} s^2 n_s(t)$. Following the convention, it behaves as $\langle s\rangle\sim|t-t_c|^{-\gamma}$. We estimate that $\gamma=1.131(6)$ in Fig. 3.14. The obtained exponent values $\beta=0.133$ and $\gamma=1.133$ satisfy the scaling relation $\beta=(\tau-2)/\sigma$ and $\gamma=(3-\tau)/\sigma$, respectively.

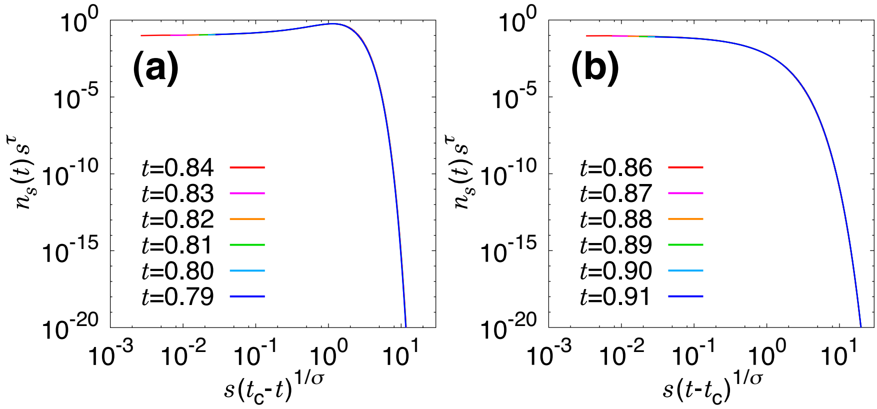

Fig. 3.12: (Color online) For static networks with $m = 3$, scaling plot of $n_s(t)s^\tau$ versus $s|t-t_c|^{1/\sigma}$ for different t that are (a) less and (b) greater than t_c. Taking $\tau = 2.105(5)$ and $\sigma = 0.790(1)$, the data for different t values look collapsed onto a single curve.

3.4 Static network model with general m

We extend the rate equation for $m = 3$ to an arbitrary value of m as follows:

$$
\begin{aligned}
&N\frac{dn_s}{dt} \\
&= \sum_{r=1}^{m-1} m\binom{m-1}{r-1} \sum_{i+j=s;i<j} in_i\left(jn_j\right)^{m-r}\left(c_{j+1}\right)^{r-1} \\
&+ \sum_{r=1}^{m-1}\binom{m}{r-1}\left(\frac{s}{2}n_{\frac{s}{2}}\right)^{m-(r-1)}\left(c_{\frac{s}{2}+1}\right)^{r-1} \\
&- 2\sum_{r=2}^{m}\binom{m}{r}\left(sn_s\right)^r\left(c_{s+1}\right)^{m-r} - m\left(sn_s\right)\left(c_{s+1}\right)^{m-1} \\
&- \sum_{r=1}^{m-1} m\binom{m-1}{r}\left(1-c_s\right)\left(sn_s\right)^r\left(c_{s+1}\right)^{m-1-r},
\end{aligned}
\tag{3.4}
$$

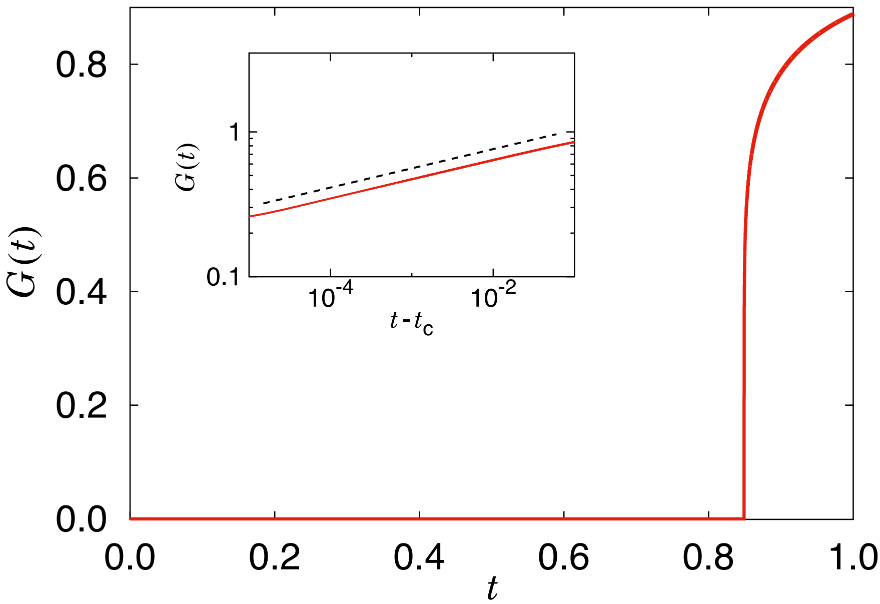

Fig. 3.13: (Color online) For static networks with $m = 3$, plot of the order parameter $G(t)$ as a function of t. Inset : The dashed line is a guide line with slope $0.133(1)$.

where the second term of the right hand side is valid only when s is an even number.

Taking similar steps used for $m = 3$, we determine the transition points and critical exponent β for general m up to $m = 15$. We determine empirically that these values behave asymptotically like $1-t_c \approx \exp(-0.59m)$ and $\beta \approx \exp(-0.70m)$, respectively. This conjecture was alluded to in [25, 26]. A numerical test is shown in Fig. 3.15.

Furthermore, we determine the exponent values τ and σ for $m = 4$ and $m = 5$ because of the instability of the cluster size distribution when the exponents τ and σ are calculated in the vicinity of $\tau = 2$. The obtained values are listed in Table 3.2. Notice that that the values approximate the formulas $\tau = 2+\beta/[1+(m-1)\beta]$ and $1/\sigma = 1+(m-1)\beta$, as shown in

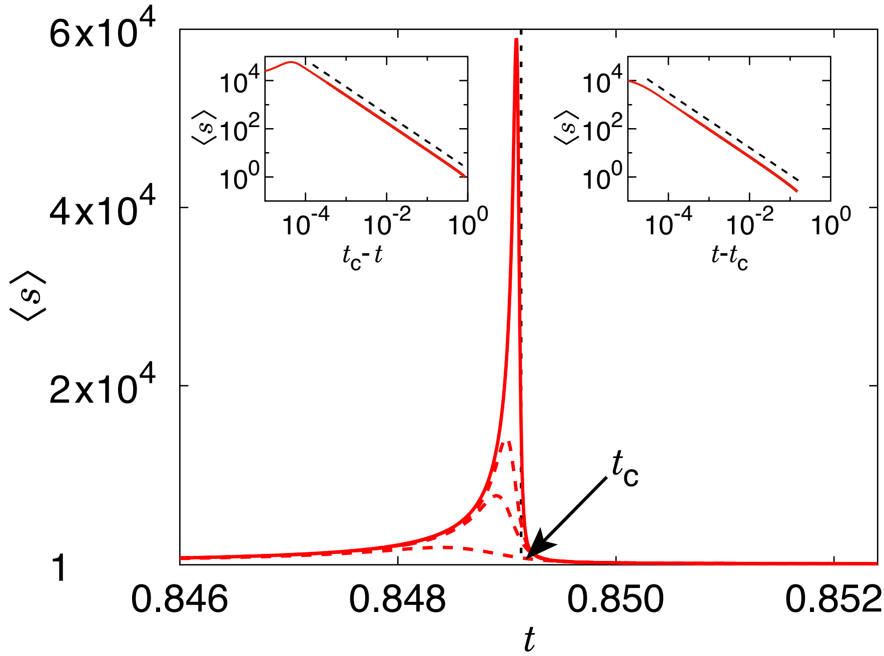

Fig. 3.14: (Color online) For static networks with $m = 3$, plot of $\langle s \rangle$ as a function of t. Inset : Plot of the susceptibility, the mean cluster size as a function of t for $t > t_c$ (right) and $t < t_c$ (left). The dashed lines are guide lines with slope $-1.131(6)$.

Fig. 3.16. This conclusion is based on a previous analytic solution to the model in [25, 26]. Due to a slight difference in the dynamic rule, the value of m in our model corresponds to $2m$ in [25, 26]; thus, the analytic solution in [25, 26] is valid for our model by replacing $2m$ with m. This allows us to obtain $\gamma = 1 + (m-2)\beta$.

Table. 3.2: Numerical estimates of the percolation threshold t_c, exponent of the cluster size distribution τ, exponent of the characteristic cluster size σ, exponent of the order parameter β, and exponent of the susceptibility γ of the static network model for $m = 2, \ldots, 5$. τ^* and β^* were obtained from $\tau^* = 2+\beta/[1+(m-1)\beta]$ and $\beta^* \approx 0.465\exp(-0.70m)$, respectively.

m	t_c	τ^*	τ	σ	β^*	β	γ
2	0.5	2.5	2.5	0.5	1	1	1
3	0.849130(1)	2.105	2.105(1)	0.790(1)	0.057	0.133(1)	1.131(6)
4	0.939678(1)	2.037	2.037(1)	0.890(1)	0.028	0.042(1)	1.082(6)
5	0.972672(1)	2.016	2.015(2)	0.940(1)	0.014	0.017(1)	1.050(4)

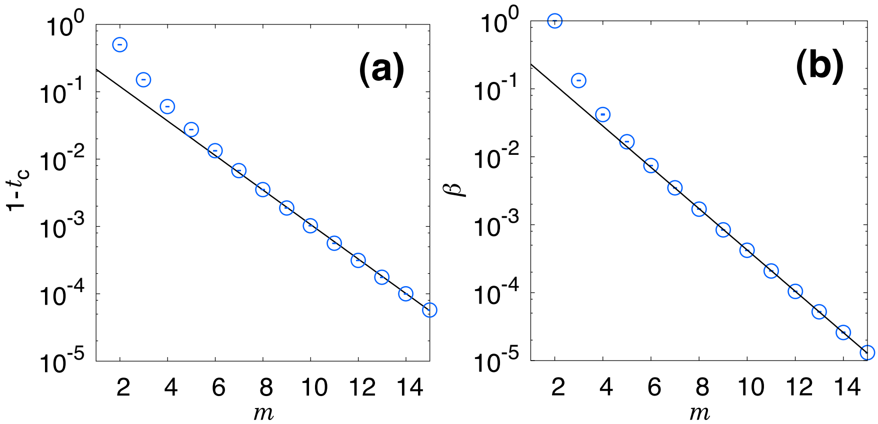

Fig. 3.15: (Color online) For static networks, (a) plot of $1-t_c$ versus m on a semi-logarithmic scale. (b) Plot of the estimated values of the exponent β for general m versus m on a semi-logarithmic scale. Asymptotically, the data points likely lie on a straight line. The error bars are smaller than the symbol sizes.

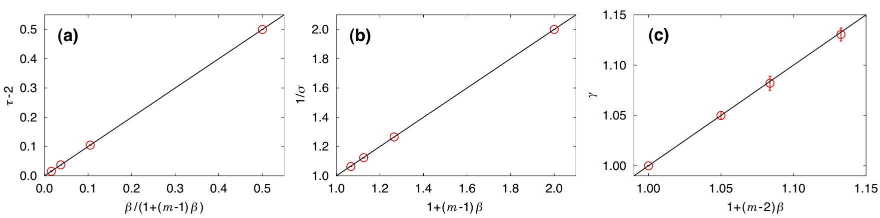

Fig. 3.16: (Color online) For static networks, formula testing for the exponents of (a) the cluster size distribution τ, (b) the characteristic cluster size σ, and (c) the mean cluster size γ, where the numerical data is obtained from the rate equation. Note that the data fit reasonably to the straight line predicted by the formula.

Chapter 4

Monte Carlo simulations

4.1 Growing network model with $m = 3$

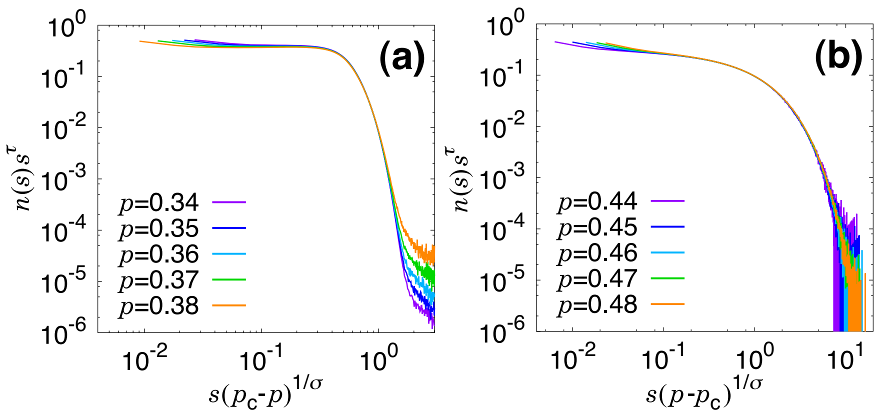

Fig. 4.17: (Color online) To obtain τ and σ by Monte Carlo simulations for growing networks, scaling plot of $n_s(p)s^\tau$ versus $s|p-p_c|^{1/\sigma}$. Data are collapsed onto a single curve by choosing $\tau = 2.5$ and $\sigma = 0.72$ for (a) $p < p_c$ and (b) $p > p_c$.

To determine the exponents τ and σ for the cluster size distribution, we numerically perform Monte Carlo simulations of the growing network models for different system sizes $N/10^4 = 2^3 - 2^{10}$; the ensemble average is taken over 10^4 configurations.

We first examine the cluster size distribution for several values of p around the transition point p_c in Fig. 4.17. The cluster size distribution follows power law at p_c and exhibits crossover behavior of $n_s(p) \sim s^{-\tau} \exp(-s|p-p_c|^{1/\sigma})$ [31, 32]. We determine $p_c = 0.4138(2)$ using the criteria that at p_c,

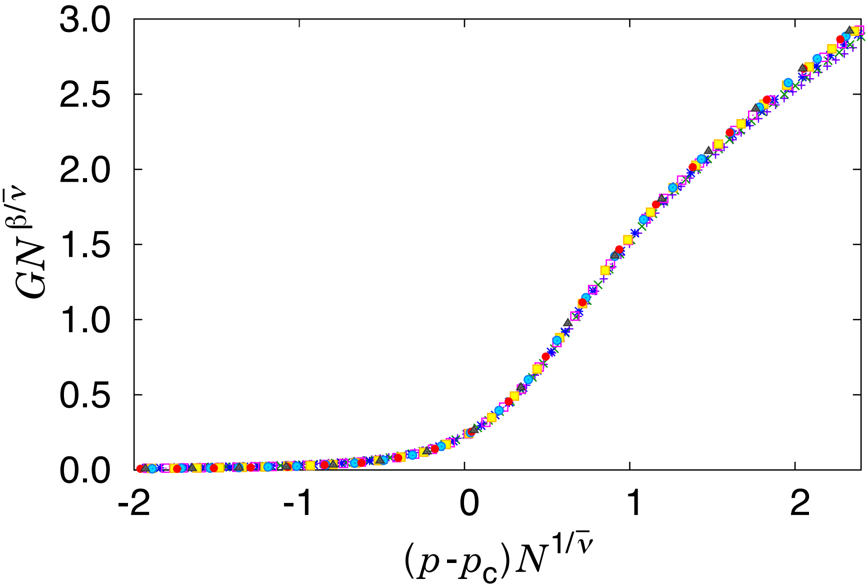

Fig. 4.18: (Color online) To obtain β by Monte Carlo simulations for growing networks, scaling plot of $GN^{\beta/\bar{\nu}}$ versus $(p-p_c)N^{1/\bar{\nu}}$ for system sizes $N/10^4 = 2^3 - 2^{10}$. Data are collapsed onto a single curve with the values of $1/\bar{\nu} = 0.35(3)$ and $\beta/\bar{\nu} = 0.24(3)$.

$n_s(p_c)$ decays in a power-law way and the relative size of the largest cluster, $G_N(p)$, follows a power law, $G \sim N^{-\beta/\bar{\nu}}$. Using the data-collapse method, we determine the exponent values of τ and σ to be $\tau \approx 2.5$ and $\sigma \approx 0.72$, respectively, which are in good agreement with the values obtained by the rate equation approach.

By measuring the exponent of the power-law behavior of $G_N(p)$ and using a finite-size scaling formula $G_N(p) = N^{-\beta/\bar{\nu}} f((p-p_c)N^{1/\bar{\nu}})$, we determine the ratios $\beta/\bar{\nu} = 0.24(3)$ and $1/\bar{\nu} \approx 0.35(3)$, as shown in Fig 4.18. We determine an exponent value of $\beta \approx 0.69$. These values are consistent with those obtained from the rate equations.

The susceptibility is also examined by plotting it in scaling form, i.e.,

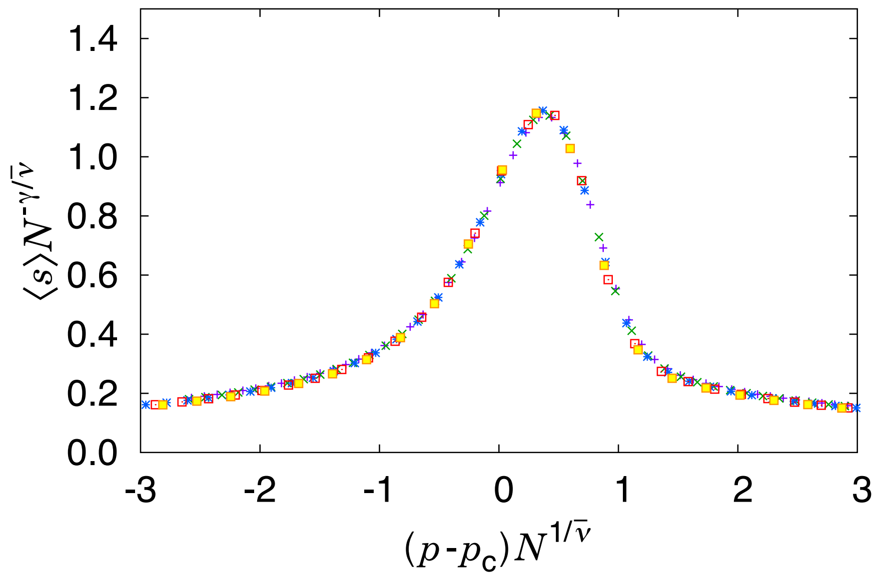

Fig. 4.19: (Color online) To obtain the exponent γ using Monte Carlo simulations for growing networks, data collapse plot of $\langle s\rangle N^{-\gamma/\bar{\nu}}$ versus $(p-p_c)N^{1/\bar{\nu}}$ for the system sizes $N/10^4 = 2^6 - 2^{10}$ in growing networks. The exponent values are $\gamma = 0.696$ and $1/\bar{\nu} = 0.35$.

$\langle s\rangle N^{-\gamma/\bar{\nu}}$ versus $(p-p_c)N^{1/\bar{\nu}}$ with $\gamma = 0.696$ and $1/\bar{\nu} = 0.35$ in Fig. 4.19 for different sizes $N/10^4 = 2^6 - 2^{10}$; the ensemble average is taken over 10^4 configurations. Notice that the data are well collapsed. This means that the hyperscaling relation $\bar{\nu} = 2\beta + \gamma$ does not hold.

4.2 Static network model with $m = 3$

To determine the exponents τ and σ for the cluster size distribution, we numerically perform Monte Carlo simulations of the static network models for different system sizes $N/10^4 = 2^0 - 2^{10}$. The ensemble average is taken over 10^5 for each data point. The cluster size distributions $n_s(t)$ for differ-

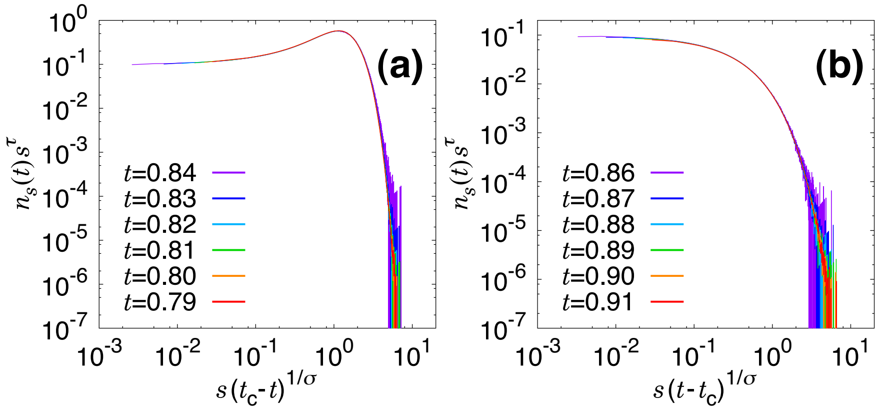

Fig. 4.20: (Color online) To obtain the exponents γ and σ using Monte Carlo simulations for static networks, data collapse plots of the rescaled cluster size distribution $n_s(t)s^{\tau}$ versus $s|t-t_c|^{1/\sigma}$ for different time steps when (a) $t < t_c$ and (b) $t > t_c$, where $\tau = 2.105$ and $\sigma = 0.79$.

ent times are plotted in scaling form, i.e., $n_s(t) \sim s^{-\tau} \exp(-s|t-t_c|^{1/\sigma})$, as shown in Fig. 4.20. Using the previously obtained values $t_c = 0.84913(1)$ and $\tau \approx 2.1$, we determine that the data for different t are well collapsed onto a single curve with $\sigma \approx 0.79$.

Next, we consider the order parameter $G(t)$ as a function of the time step t for different sizes $N/10^4 = 2^0 - 2^{10}$. The critical point t_c and critical exponent β are determined using the scaling ansatz $G_N(t) = N^{-\beta/\bar{\nu}} f((t-t_c)N^{1/\bar{\nu}})$. Using the criterion that $G_N(t) \sim N^{-\beta/\bar{\nu}}$ at $t = t_c$, we determine $t_c = 0.84913(1)$ and $\beta/\bar{\nu} \approx 0.06$ in Fig. 4.21. Moreover, all of the data for different system sizes are systematically collapsed onto a single curve when $1/\bar{\nu} \approx 0.45$, as shown in Fig. 4.21. This suggests that $\beta \approx 0.133$. The value of β is consistent with the results obtained by the rate equation approach.

Finally, we study the susceptibility behavior as a function of the time step. The susceptibility is also examined by plotting it in scaling form, i.e.,

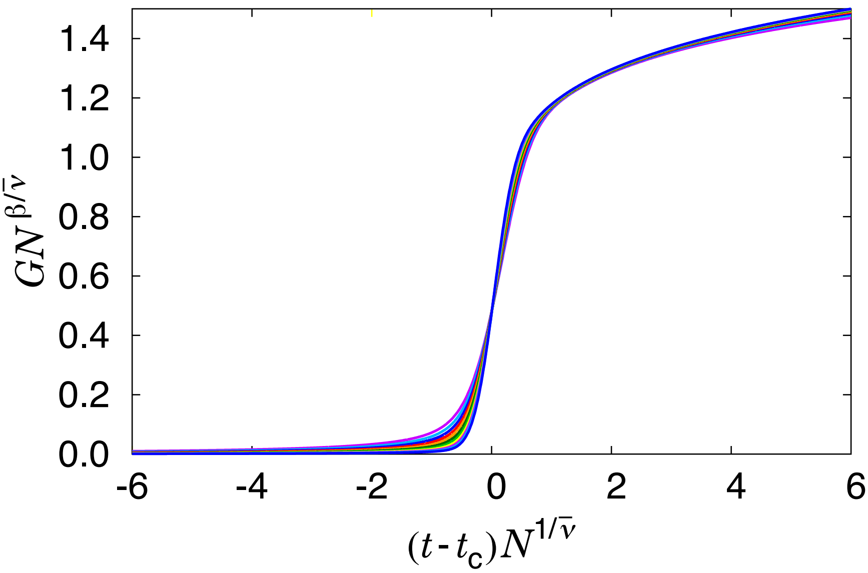

Fig. 4.21: (Color online) To obtain β using Monte Carlo simulations for static networks, data collapse plot of $GN^{\beta/\bar{\nu}}$ versus $(t-t_c)N^{1/\bar{\nu}}$ for system sizes $N/10^4 = 2^0 - 2^{10}$. Data for different values of N are systematically collapsed near the transition point by taking $1/\bar{\nu} = 0.45$ and $\beta/\bar{\nu} = 0.06$.

$\langle s\rangle N^{-\gamma/\bar{\nu}}$ versus $(t-t_c)N^{1/\bar{\nu}}$ with $\gamma = 1.133$ and $1/\bar{\nu} = 0.45$ in Fig. 4.22. Notice that the data are well collapsed. This means that the hyperscaling relation $\bar{\nu} = 2\beta + \gamma$ doe not hold.

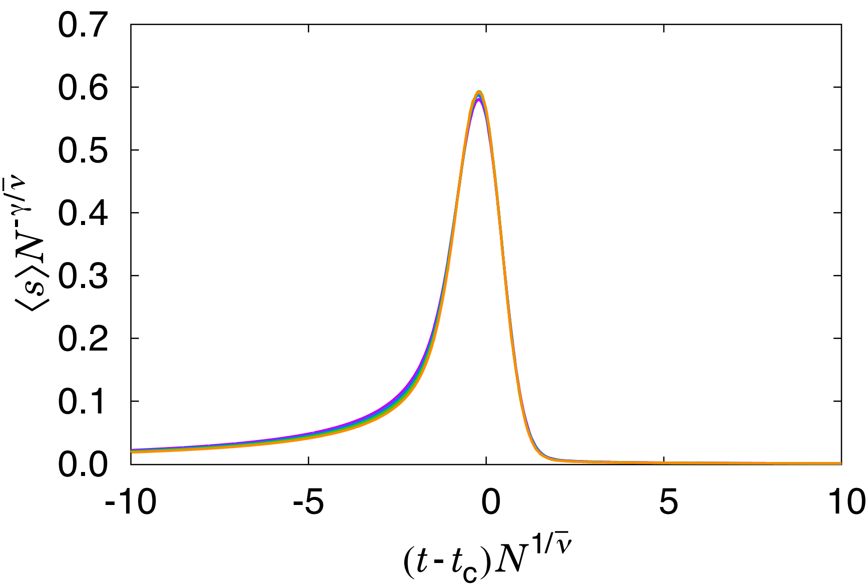

Fig. 4.22: (Color online) To obtain γ using Monte Carlo simulations for static networks, data collapse plot of $\langle s\rangle N^{-\gamma/\bar{\nu}}$ versus $(t-t_c)N^{1/\bar{\nu}}$ for system sizes $N/10^4 = 2^7 - 2^{10}$, where the exponent values $\gamma = 1.133$ and $1/\bar{\nu} = 0.45$ are used.

Chapter 5

Comparison of $n_s(p)$ for growing network models

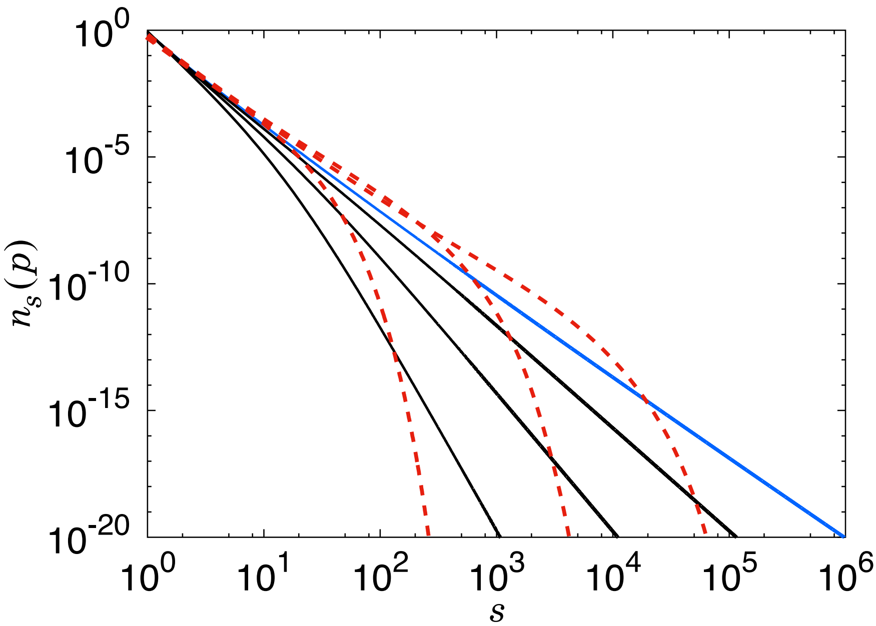

Fig. 5.23: (Color online) For growing network with $m = 2$, plot of $n_s(p)$ versus s at $p = p_c$ (blue solid line), $p > p_c$ (red dashed line), and $p < p_c$ (black solid line) based on the numerical values obtained from the rate equation. The transition point is $p_c = 0.125$. For $p \leq p_c$, $n_s(p)$ decays in a power-law manner, indicating that the transition is infinite-order.

It is interesting to note that the percolation occurring in growing network models when $m \geq 3$ is a second-order phase transition, whereas it is of infinite order when $m = 2$. We investigate the cluster size distribution $n_s(p)$

for $m = 2$. As shown in Fig. 5.23, $n_s(p)$ decays in a power-law way when $p \le p_c$, while it exhibits crossover behavior when $p > p_c$. The power-law behavior of $n_s(p)$ when $p \le p_c$ implies that the region $p \le p_c$ is the critical phase, which is noticeable in the infinite-order transition. Intuitively, when $p \le p_c$, in the growing network, the fraction of nodes that belong to small-size clusters is relatively low compared to the fraction for the second-order phase transition model; for example, when $m \ge 3$ in Fig. 3.5. However, when $m \ge 3$, the density of large-size clusters is suppressed by the Achlioptas rule, which leads to crossover behavior even for $p < p_c$. Thus, the percolation transition in growing networks for $m \ge 3$ is second order.

Chapter 6

Summary and discussion

In our minimal model that incorporates both growing and static Achlioptas processes, the results obtained from the rate equations and Monte-Carlo simulations for the cluster size distribution are consistent. When $m = 2$, the growing and static models correspond to the Callaway random growing model [14] and Erdős-Rényi model [29], respectively.

In the growing network model, as m increases from 2 to 3, the transitional nature of percolation changes from infinite-order to second-order due to the Achlioptas process [16]. On the other hand, in the static model, the order of the phase transition is the same as that of the second-order ER model, but the order parameter exponent β decreases exponentially as m increases and the transition becomes more explosive. The Achlioptas process rule leads to the suppression effect against the growth of large clusters, which causes the cluster size distribution in large-cluster regions to decay exponentially; thus, the transition is second-order.

Moreover, in this paper, we showed that the critical exponent β decreases algebraically with m in growing networks; however, it decays exponentially in static networks. This fact reflects that the suppression effect in growing networks is weaker than that in static networks. Furthermore, we obtained the critical exponents and their tendencies in both growing and static models for arbitrary values of m. We also found that the m-

dependent exponents always satisfy the scaling relations $\beta = (2-\tau)/\sigma$ and $\gamma = (3-\tau)/\sigma$ [1, 2]. However, the hyperscaling relation $\bar{\nu} = 2\beta + \gamma$ does not hold in both growing and static networks. We expected $\bar{\nu} \approx 2.08$ from the relation $2\beta + \gamma$ for the growing networks of $m = 3$, but obtained $\bar{\nu} \approx 2.86$ $(1/\bar{\nu} = 0.35)$ from Monte Carlo simulations. For the static network with $m = 3$, we expected $\bar{\nu} \approx 1.4$ $(1/\bar{\nu} = 0.71)$, but obtained $\bar{\nu} = 2.22$ $(1/\bar{\nu} = 0.45)$. The origin of these inconsistencies are still not clear. We remark that the failure of the hyperscaling relation $\bar{\nu} = 2\beta + \gamma$ was also observed in the previous research of Achlioptas process [33].

Bibliography

[1] D. Stauffer, Phys. Rep. **54**, 1 (1979).

[2] D. Stauffer and A. Aharony, *Introduction to percolation Theory* (Taylor and Francis, London, 1994).

[3] P. J. Flory, J. Am. Chem. Soc. **63**, 3083 (1941).

[4] S. R. Broadbent and J. M. Hammersley, Proc. Cambridge Philos. Soc. **53**, 629 (1957).

[5] E. M. Hendriks, M. H. Ernst, and R. M. Ziff, J. Stat. Phys. **31**, 519 (1983).

[6] F. Leyvraz, Phys. Rep. **383**, 95 (2003).

[7] P. Grassberger, Math. Boisci. **63**, 157 (1983).

[8] D. Mollison, J. R. Statist. Soc. B **39**, 283 (1977).

[9] J. D. Murray, *Mathematical Biology* (pringer, Berlin, 2005).

[10] J. L. Cardy and P. Grassberger, J. Phys. A: Math. Gen. **18**, L267 (1985).

[11] M. Walther, D. G. Cooke, C. Sherstan, M. Hajar, M. R. Freeman, and F. A. Hegmann, Phys. Rev. B **76**, 125408 (2007).

[12] S. Boettcher, V. Singh, and R. M. Ziff, Nat. Comm. **3**, 787 (2012).

[13] J. Kim, P.L. Krapivsky, B. Kahng, and S. Redner, Phys. Rev. E **66**, 055101(R) (2002).

[14] Duncan S. Callaway, John E. Hopcroft, Jon M. Kleinberg, M. E. J. Newman, and Steven H. Strogatz, Phys. Rev. E **64**, 041902 (2001).

[15] J. Chalupa, P.L. Leath, and G.R. Reich, J. Phys. C **12**, L31 (1979).

[16] D. Achlioptas, R. M. D'Souza, and J. Spencer, Science **323**, 1453 (2009).

[17] J. Adler, Physica A **171**, 453 (1991).

[18] S.N. Dorogovtsev, A.V. Goltsev, J.F.F. Mendes, Phys. Rev. Lett. **96**, 040601 (2006).

[19] B. Bollobás, *Graph Theory and Combinatorics: Proc. Cambridge Combinatorial Conference in Honour of Paul Erös* (Academic Press, New York, Berlin, 1984).

[20] S. V. Buldyrev, R. Parshani, G. Paul, H. E. Stanley and S. Havlin, Nature **464**, 1025 (2010).

[21] S.-W. Son, P. Grassberger and M. Paczuski, Phys. Rev. Lett. **107**, 195702 (2011).

[22] Y. S. Cho, S. Hwang, H. J. Herrman and, B. Kahng, Science **339**, 1185 (2013).

[23] J. Gómez-Gardénes, S. Gómez, A. Arenas and Y. Moreno, Phys. Rev. Lett. **106**, 128701 (2011).

[24] P. Echenique, J. Gómez-Gardeńes and Y. MorenoEurophys. Lett. **71**, 325 (2005).

[25] R. A. da Costa, S. N. Dorogovtsev, A. V. Goltsev, and J. F. F. Mendes, Phys. Rev. E **89**, 042148 (2014).

[26] R. A. da Costa, S. N. Dorogovtsev, A. V. Goltsev, and J. F. F. Mendes, Phys. Rev. E **90**, 022145 (2014).

[27] R. A. da Costa, S. N. Dorogovtsev, A. V. Goltsev, and J. F. F. Mendes, Phys. Rev. Lett. **105**, 255701 (2010).

[28] B. Bollobás, *Random Graphs* (Academic Press, New York, 1985).

[29] P. Erdős and A. Rényi, Publ. Math. Inst. Hungar. Acad. Sci. A **5**, 17 (1960).

[30] R. M. D'Souza and M. Mitzenmacher, Phys. Rev. Lett. **104**, 195702 (2010).

[31] K. Christensen and N. R. Moloney, *Complexity and Criticality* (World Scientific Pub Co Inc, 2005).

[32] F. Radicchi and S. Fortunato, Phys. Rev. E **81**, 036110 (2010).

[33] P. Grassberger, C. Christensen, G. Bizhani, S.-W. Son, and M. Paczuski, Phys. Rev. Lett. **106**, 225701 (2011).

초 록

최근 폭발적 여과 상전이 모델(EP 모델)에 대한 많은 연구들이 행해지고 있다. 이러한 연구들로 인해 EP 모델이 0(불연속 1차 상전이)이 아닌 매우 작은 양의 β 값을 갖는 연속 상전이(2차상전이) 모델이라는 것이 밝혀졌다. 이는 네트워크의 전체 노드의 개수가 시간에 따라 변하지 않는 정적 네트웨크에서 얻어진 결과들이다. 하지만, 실제 사회 네트워크를 구성하는 구성원들 중에서 거대한 구성요소가 빠르게 자라나는 사회 네트워크는 특정 시간 간격마다 네트워크를 구성하는 전체요소(노드)의 수가 증가하는 성장하는 네크워크에 해당 될 수 있다. 그러므로 우리는 이러한 성장하는 네트워크에서 발생하는 폭발적 여과 상전이에 대해서 연구할 필요성을 느꼈다. 이에 우리는 매 초마다 선택되는 후보 노드의 개수가 m 개인 일반적인 경우에 대해서 연구를 해 보고자 하였다. 후보 노드개수 m 이 2 일 때, 본 연구의 모델은 과거 Callaway 등에 의해 연구가 진행 되었던 무한차 상전이를 겪는 보통의 임의로 성장하는 네트워크 모델이 된다. 하지만, 우리는 후보 노드개수 m이 3 이상이 되면 본 모델은 거대한 클러스터의 생성을 억제하는 아클리옵타스 과정에 의한 효과로 인하여 연속 상전이(2차 상전이)를 겪게 된다는 것을 알아 내었다. 그리고 이러한 성장하는 네트워크에서의 클러스터 크기 분포에 대한 비율 방정식과 몬테칼로 시뮬레이션을 이용하여, 후보 노드 개수 m이 증가할수록 임계 계수 β가 지수적으로 감소하였던 정적 네트워크의 경우와는 달리 성장하는 네트워

크에서는 대수적으로 감소한다는 것을 보였다.

주요어 : 여과 상전이, 여과 클러스터, 폭발적인 여과 상전이, 불연속 여과 상전이, 아클리옵타스 과정 , 유한 크기 축적 이론

학번 : 2012-20372